

Enhanced Thermoelectric Properties of Hydrothermal Synthesized BiCl₃/Bi₂S₃ Composites

WANG Wei¹, LUO Shi-Jie¹, XIAN Cong¹, XIAO Qun¹, YANG Yang², OU Yun³, LIU Yun-Ya¹, XIE Shu-Hong⁴

(1. Hunan Provincial Key Laboratory of Thin Film Materials and Devices, School of Materials Science and Engineering, Xiangtan University, Xiangtan 411105, China; 2. Department of Mechanical Engineering, University of Washington, Seattle WA 98195-2600, USA; 3. Hunan Provincial Key Laboratory of Health Maintenance for Mechanical Equipment, Hunan University of Science and Technology, Xiangtan 411201, China; 4. Key Laboratory of Low Dimensional Materials and Application Technology of Ministry of Education, Xiangtan University, Xiangtan 411105, China)

Abstract: Hierarchical spherical Bi₂S₃ particles with nanorod were synthesized by hydrothermal method, and then BiCl₃/Bi₂S₃ composite powders with different molar ratios were consolidated into bulk samples by spark plasma sintering (SPS) technique. The addition of BiCl₃ with appropriate amount not only increased the electrical conductivity, but also decreased the thermal conductivity of Bi₂S₃. The Bi₂S₃ sample doped with 0.5mol% BiCl₃ shows a maximum electrical conductivity of 45.1 S·cm⁻¹ at 762 K, which is much higher than that of pure Bi₂S₃ at 762 K (12.9 S·cm⁻¹). The minimum thermal conductivity is 0.31 W·m⁻¹·K⁻¹ for the Bi₂S₃ sample doped with 0.25mol% BiCl₃ at 762 K, which is lower than that of pure Bi₂S₃ (0.47 W·m⁻¹·K⁻¹) at the same temperature. The maximum *ZT* value of 0.63 at 762 K was achieved by Bi₂S₃ doped with 0.25mol% BiCl₃, which is almost two times higher than that of pure Bi₂S₃ (0.22).

Key words: Bi₂S₃; hydrothermal method; spherical particle; spark plasma sintering; thermoelectric

Thermoelectric (TE) materials have attracted more and more attention as they can convert heat into electricity directly^[1-3]. The performance of thermoelectric materials depends on the figure of merit *ZT*, which is given by $ZT = S^2 \sigma T / (\kappa_e + \kappa_{lat})$, where *S*, σ , *T*, κ_e and κ_{lat} are Seebeck coefficient, electrical conductivity, absolute temperature, carrier thermal conductivity and lattice thermal conductivity, respectively^[1]. It is obvious that high efficiency thermoelectric conversion requires high power factor ($S^2 \sigma$) and low thermal conductivity simultaneously. However, the parameters mentioned above are coupled together and depend on the carrier concentrations, it is difficult to control the parameters independently. As such, many techniques have been used to enhance the *ZT*, such as nanostructures^[4], layered thermoelectric materials^[5-7], atomic substitution in alloys^[8-9]. At the same time, many methods and theories were developed for analyzing the thermoelectric properties of composite materials, such as SThM^[10], mesomechanics combined phase field simulation^[11], and nonlinear asymptotic homogenization theories^[12]. Thermoelectric

materials are also combined with other energy technologies to achieve more application prospect, such as thermoelectric hybrid battery system^[13].

Among thermoelectric materials, the Pb-Te based^[14-15] and Bi-Te based^[16-17] compounds are the most promising candidates for TE applications. However, the rareness and high expense of tellurium have limited their application. Thus it is necessary to develop alternative materials that are abundant and cheaper. Bismuth sulfide (Bi₂S₃) has recently attracted much attention for its potential application in thermoelectric field. Bi₂S₃ has low thermal conductivity and high Seebeck coefficient at room temperature, though its electrical resistivity is high^[18-20]. Thus the key point for improving the thermoelectric performance of Bi₂S₃ is to reduce the electrical resistivity^[21]. In order to reduce the electrical resistivity of Bi₂S₃, several experimental methods have been reported, such as adding one-dimensional nanorods into Bi₂S₃ films^[17,22], and Cu or Ag doping^[23-24]. In this study, the TE properties of Bi₂S₃ are enhanced by doping with BiCl₃, for BiCl₃ as an electron donor dopant can improve the carrier content and increase the electrical conductivity^[25].

Received date: 2018-06-11; Modified date: 2018-09-14

Foundation item: National Natural Science Foundation of China (11627801, 51772254, 11702092); Scientific Research Fund of Hunan Provincial Education Department (16A202)

Biography: WANG Wei (1988-), male, candidate of PhD. E-mail: yuhong138@163.com

Corresponding author: XIE Shu-Hong, professor. E-mail: shxie@xtu.edu.cn

1 Experimental procedure

Bi(NO₃)₃·5H₂O and thiourea were used as the raw materials to synthesize the Bi₂S₃ powders. In the typical hydrothermal synthesis, 1.5 g Bi(NO₃)₃·5H₂O and 1.5 g thiourea were dissolved in 40 mL deionized water with continuous stirring, and then transferred to a Teflon-lined stainless-steel autoclave with a capacity of 50 mL. After that the hybrid solution was maintained at 180 °C for 24 h, then it was air-cooled to room temperature. The synthesized precipitates of Bi₂S₃ were filtered and washed with distilled water and ethanol, and dried in air at 60 °C. Afterwards, appropriate amounts of commercial BiCl₃ (99.99%, Alfa Aesar) and Bi₂S₃ powders with different molar ratios were mixed in 40 mL ethylalcohol with stirring for 2 h, and the molar ratios of BiCl₃ were controlled to be 0, 0.25%, 0.5% and 1.0%, respectively. They were sonicated for 30 min, and then the sample was dried in vacuum oven at 60 °C. Different composite powders were loaded into a graphite die with an inner diameter of 12.6 mm and then sintered at 723 K for 10 min at a heating rate of 100 K/min under an axial compressive stress of 45 MPa in vacuum by using a spark plasma sintering (SPS) system (SPS-211LX). The SPSed specimens were disk-shaped with dimensions of 12.6 mm×4 mm.

The phase structure was analyzed by X-ray diffraction (XRD) with graphite monochromatized Cu K α radiation ($\lambda=0.15418$ nm) (D/max-rA). The morphologies of the powders and the bulk samples after SPS were observed by field-emission scanning electron microscopy (FESEM, LEO-1525), and transmission electron microscopy (TEM, JEM-2100).

Thermoelectric properties were measured with specimen surface perpendicular to the pressing direction of SPS. Seebeck coefficient and electrical resistivity were measured by Seebeck coefficient/electric resistance measuring system (ZEM-3). The thermal conductivity was calculated from the product of measured thermal diffusivity, specific heat and density. The thermal diffusivity was measured by the flash method (LFA427, NETZSCH). Before measurement, the sample was coated with a thin layer of graphite by graphite spray (Graphite33) to improve the thermal homogeneity of the sample. The specific heat capacity C_p was determined by differential scanning calorimetry (DSC 404F3, NETZSCH), which is in the range of 0.24–0.29 J·g⁻¹·K⁻¹ between room temperature and 750 K. The density was measured by Archimedes method. The thermal conductivity was calculated *via* the equation $\kappa=\rho DC_p$ (κ is the thermal conductivity, ρ is the density, D is the thermal diffusivity, and C_p is the specific heat capacity). Hall coefficients were measured on a home-built system with magnetic

fields in the range of 0–1.25 T, utilizing a simple four-contact Hall-bar geometry in both negative and positive polarity to eliminate Joule resistive errors.

2 Results and discussion

Figure 1(a) shows the XRD patterns of BiCl₃/Bi₂S₃ composite powders with different xmol% ($x=0, 0.25, 0.5$, and 1.0) BiCl₃. The results show that all the patterns correspond to the orthorhombic Bi₂S₃, indicating that the main phase of all the samples is Bi₂S₃ without preferred orientation, and no obvious impurity phases are observed as the content of BiCl₃ no more than 1.0mol%. The enlarged patterns of 2θ in the range of 24°–32.5° are shown in Fig. 1(b). The ionic radius of Cl⁻ is 0.181 nm, which is slightly smaller than that of S²⁻ (0.184 nm), so the substitution of S²⁻ with Cl⁻ induces a slight shrinkage of the unit cell, which results in the refined right shift of the major diffraction peaks with BiCl₃ doping^[25]. According to the bond-order-length-strength (BOLS) theory, the fine nanocrystal can effectively decrease the average lattice constant of material^[26], thus the shift of the major diffraction peaks for the doped materials is a combined result of both grain size and solid solubility. The major diffraction peaks should shift towards more right with increasing the solid solubility of BiCl₃, however, corresponding average

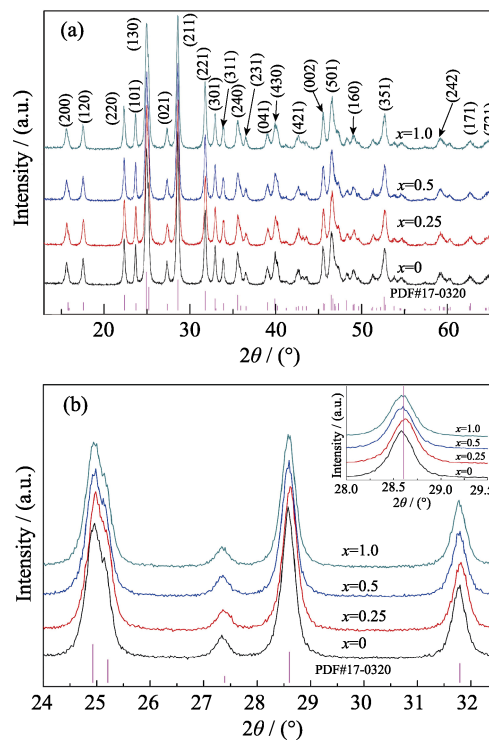


Fig. 1 XRD patterns (a) and the enlarged patterns of 2θ in the range of 24°–32.5°(b) with peaks of crystal plane (211) in the inset for BiCl₃/Bi₂S₃ powders with different xmol% ($x=0, 0.25, 0.5$, and 1.0) BiCl₃

grain size change simultaneously. The final result is that the sample doped with 0.25mol% BiCl₃ has the largest right shift among all specimens, as shown in the inset of Fig. 1(b), which is primarily due to the smallest grain size, and later SEM results will reveal it.

The FESEM images of Bi₂S₃ powders and fractured surfaces of sintered samples of Bi₂S₃ doped with *x*mol% BiCl₃ (*x*=0, 0.25, 0.5, 1.0) and TEM images of Bi₂S₃ doped with *x*mol% (*x*= 0, 1.0) BiCl₃ after SPS are shown in Fig. 2. It is observed in Fig. 2(a) that the major morphology of Bi₂S₃ powders synthesized by the hydrothermal method are spherical with diameter around 3–4 μm and the spherical particles are hierarchical, consisting of fine Bi₂S₃ nanorods with diameter in the range of 100–200 nm and length in the range of 1–3 μm^[27]. Figure 2(b) shows the morphology of bulk Bi₂S₃ after SPS, showing that the grain size of the nanorods keeps stable, and the SPS sample is compact without obvious crack, though there are some small holes. The relative density of Bi₂S₃ is 89% as shown in Table 1, the theoretical density of Bi₂S₃ is 6.81 g·cm⁻³^[28]. Figure 2(c-e) show the morphologies of Bi₂S₃ doped with different BiCl₃. It is obvious that BiCl₃ doping changes the morphologies of Bi₂S₃ due to the activation role of BiCl₃ by forming a substitution solid solution with Bi₂S₃^[25]. In Fig. 2(c), the grain size of Bi₂S₃ doped with 0.25mol% BiCl₃ is inhomogeneous, many fine particles are mixed with micrometer grains, and small pores are uniformly distributed in bulk. It is observed that the grain size of Bi₂S₃ doped with 0.5mol% BiCl₃ in Fig. 2(d) is similar to that of Bi₂S₃ doped with 1.0mol% BiCl₃ in Fig. 2(e). Figure 2(f) shows the TEM image of Bi₂S₃ powders after SPS, which demonstrates that nanometer grain size is preserved after SPS. The orthorhombic structure of Bi₂S₃ is also confirmed by HRTEM, as shown in Fig. 2(g), where the lattice spacing is measured to be 0.421 nm along (220) plane and 0.357 nm along (130) plane, respectively. Figure 2(h) shows the TEM image of Bi₂S₃ doped with 1.0mol% BiCl₃ powder after SPS, which confirms that partial nanorod structure still remains, and the grain size is similar to pure Bi₂S₃. SEM image of Bi₂S₃ doped with 1.0mol% BiCl₃ bulk after SPS and corresponding elemental mappings of Bi, S and Cl are shown in Fig. 3. Elemental mappings reveal that the distribution of Cl element is uniform, which indicates that Bi₂S₃ doped with BiCl₃ is

a substitutional solid solution as BiCl₃ powders dispersed uniformly in Bi₂S₃ powder by alcohol ultrasonication.

Figure 4 shows the temperature dependence of thermoelectric performances for BiCl₃/Bi₂S₃ composite samples. The negative Seebeck coefficients in Fig. 4(a) indicates that the composites are n-type semiconductors and the major carriers are electrons. The Seebeck coefficient of pure Bi₂S₃ sample is about -442.0 μV·K⁻¹ at 336 K and the corresponding values of BiCl₃/Bi₂S₃ composites are in the range of -322.0 – -247.3 μV·K⁻¹. The values of carrier concentration at room temperature are displayed in Table 2, which shows that the carrier concentration increases monotonically with increasing BiCl₃

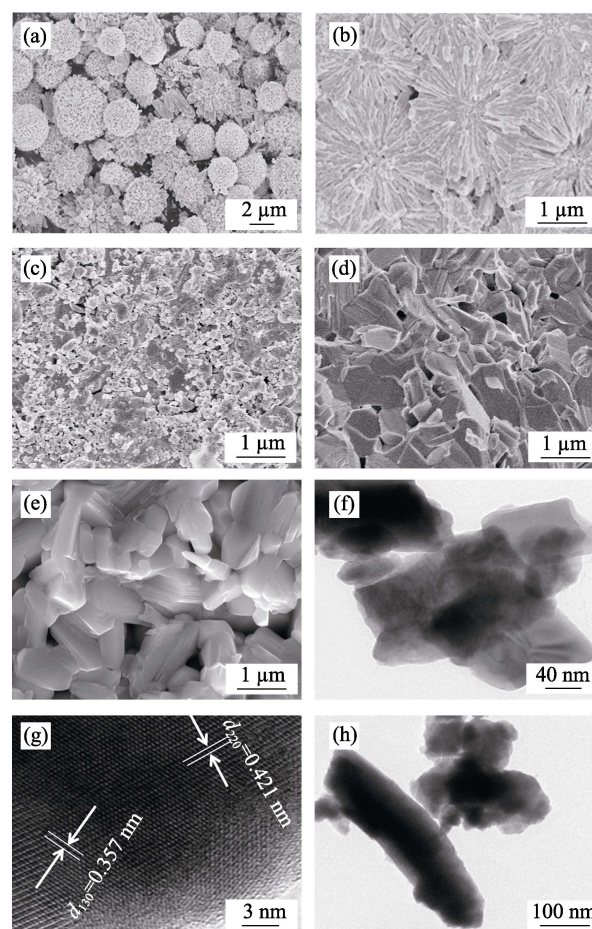


Fig. 2 SEM images of Bi₂S₃ powders (a), fractured surfaces of SPSed samples of Bi₂S₃ doped with *x*mol% BiCl₃ ((b) *x*=0, (c) *x*=0.25, (d) *x*=0.5, (e) *x*=1.0); TEM images of sintered samples of Bi₂S₃ doped with *x*mol% BiCl₃ ((f) *x*=0, (h) *x*=1.0); HRTEM image of Bi₂S₃ powder after SPS (g)

Table 1 Thermoelectric performance of BiCl₃/Bi₂S₃ samples at 762 K

Sample	ρ /%	$S/(\mu\text{V}\cdot\text{K}^{-1})$	$\sigma/(\text{S}\cdot\text{cm}^{-1})$	$PF/(\mu\text{W}\cdot\text{m}^{-1}\cdot\text{K}^{-2})$	$\kappa/(\text{W}\cdot\text{m}^{-1}\cdot\text{K}^{-1})$	ZT
Bi ₂ S ₃	89%	-326.0	12.9	136.9	0.47	0.22
Bi ₂ S ₃ +0.25% BiCl ₃	90%	-304.0	27.6	255.0	0.31	0.63
Bi ₂ S ₃ +0.5% BiCl ₃	89%	-279.0	45.1	350.2	0.58	0.46
Bi ₂ S ₃ +1.0% BiCl ₃	92%	-273.5	25.4	189.7	0.49	0.30

content. It is obvious that near room temperature Seebeck coefficient de-creases with increasing amount of BiCl₃ due to the increased carrier concentration with addition of BiCl₃^[19]. It is shown that the Seebeck coefficient of pure Bi₂S₃ decreases with increasing temperature owing to the decreasing carrier mobility with increasing temperature. But for the BiCl₃/Bi₂S₃ composite samples, Seebeck coefficient increases at lower temperature and then de-creases at higher temperature, which is probably due to the bipolar effect caused by the band gap reduction at a higher temperature^[29-30]. Figure 4(b) shows that the electrical conductivity (σ) as a whole increases with increasing temperature, and displays a semiconducting behavior. The σ of pure Bi₂S₃ is in the range of 1.0 S·cm⁻¹ to 12.9 S·cm⁻¹ at 336–762 K. The maximum σ of 45.1 S·cm⁻¹ is present in Bi₂S₃ doped with 0.5mol% BiCl₃ at 762 K. However, σ of Bi₂S₃ doped with 1.0mol% BiCl₃ increases at first and then decreases with rising temperature. According to the formula $\sigma = ne\mu$, σ of semiconductor is

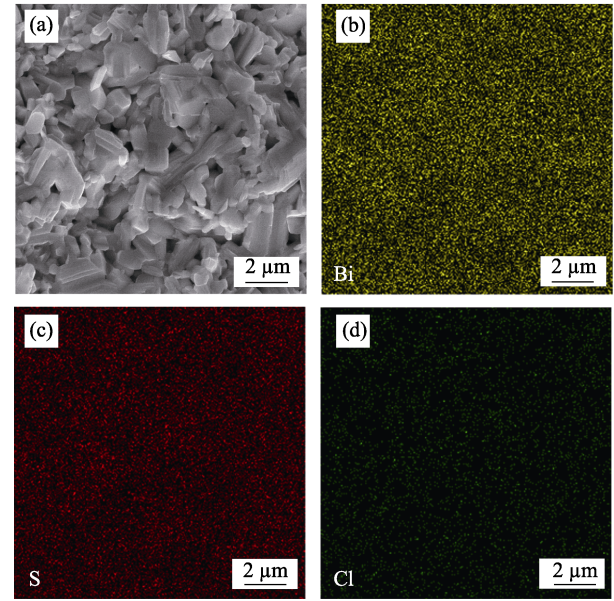


Fig. 3 SEM image of the fractured surfaces of Bi₂S₃ doped with 1.0mol% BiCl₃ bulk after SPS (a), corresponding elemental mappings of Bi, S and Cl (b-d)

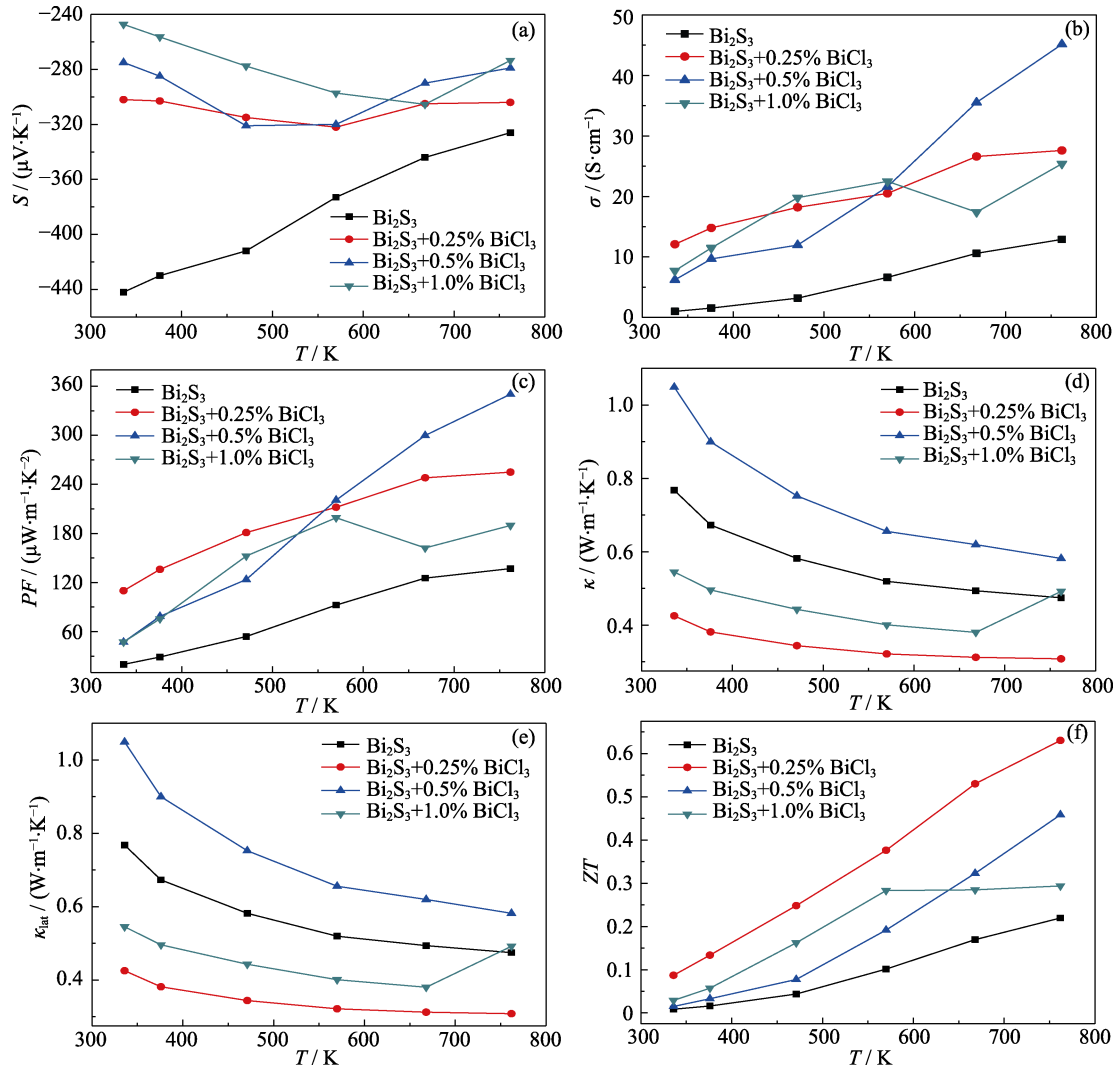


Fig. 4 Temperature dependence of thermoelectric performances for BiCl₃/Bi₂S₃ composite samples (a) Seebeck coefficient; (b) Electrical conductivity; (c) Power factor; (d) Total thermal conductivity; (e) Lattice thermal conductivity; (f) Figure of merit (ZT)

Table 2 Carrier concentration of BiCl₃/Bi₂S₃ samples at room temperature

Sample	Bi ₂ S ₃	Bi ₂ S ₃ +0.25% BiCl ₃	Bi ₂ S ₃ +0.5% BiCl ₃	Bi ₂ S ₃ +1.0% BiCl ₃
Carrier concentration/($\times 10^{15}$, cm ⁻³)	1.82	2.13	4.31	6.83

proportional to carrier concentration (n), electron charge (e) and electron mobility (μ). With the increase of temperature, more electrons are excited and the carrier concentration increases, but the electron mobility decreases due to the phonon scattering^[25], which leads to increased electrical conductivity at lower temperatures and then decreased electrical conductivity at a higher temperature for the sample doped with 1.0mol% BiCl₃. It is observed that the change of σ with different doping concentration is irregular, which is probably due to the complex absorption of hydrothermally synthesized powders. The power factor ($S^2\sigma$) is shown in Fig. 4(c). The pure Bi₂S₃ shows a minimum power factor of $19.8 \mu\text{W}\cdot\text{m}^{-1}\cdot\text{K}^{-2}$ around 336 K, and the corresponding value is $110.0 \mu\text{W}\cdot\text{m}^{-1}\cdot\text{K}^{-2}$ for Bi₂S₃ doped with 0.25mol% BiCl₃, and the highest power factor reaches $350.2 \mu\text{W}\cdot\text{m}^{-1}\cdot\text{K}^{-2}$ at 762 K for the Bi₂S₃ doped with 0.5mol% BiCl₃. It is obvious that the doped BiCl₃ enhances the power factor of Bi₂S₃.

The thermal conductivity (κ) of the samples decreases with increasing temperatures, as shown in Fig. 4(d), which is attributed to the strong phonon scattering at high temperatures. The composite sample has a lower κ than that of the pure Bi₂S₃ as the second phase BiCl₃ enhances the phonon scattering^[23]. Bi₂S₃ doped with 0.5mol% BiCl₃ has the highest σ and κ at higher temperatures probably due to the higher carrier concentration, lattice deformation and larger grain size as shown in Fig 2(d). The thermal conductivity of Bi₂S₃ doped with 1.0mol% BiCl₃ is a little lower than that of Bi₂S₃ doped with 0.5mol% BiCl₃, probably owing to a high doping fraction introducing more lattice defects, which is an effective approach for decreasing the lattice thermal conductivity, thus achieving a lower κ_{lat} ^[31]. The minimum κ is $0.31 \text{ W}\cdot\text{m}^{-1}\cdot\text{K}^{-1}$ at 762 K for Bi₂S₃ doped with 0.25mol% BiCl₃ due to the formation of many fine grains, which is 34% lower than that of pure Bi₂S₃ ($0.47 \text{ W}\cdot\text{m}^{-1}\cdot\text{K}^{-1}$). The temperature dependence of lattice thermal conductivity (κ_{lat}) is shown in Fig. 4(e). The ratio of lattice thermal conductivity (κ_{lat}) to κ_{tot} indicates that κ_{tot} is dominated by phonon transport. It is observed in Fig. 4(f) that all the samples show an increased ZT value with temperature increasing, which is attributed to the increased σ and decreased κ . It is observed in Table 1 that the maximal ZT of 0.63 at 762 K is obtained in Bi₂S₃ doped with 0.25mol% BiCl₃, which is a higher ZT compared with the reported Bi₂S₃-based material^[25, 32-34].

3 Conclusions

n-type BiCl₃/Bi₂S₃ composite samples were fabricated by hydrothermal method combined with SPS technique. The addition of BiCl₃ effectively increased the electrical conductivity and decreased the thermal conductivity of Bi₂S₃. Bi₂S₃ doped with 0.5mol% BiCl₃ shows a maximum electrical conductivity of $45.1 \text{ S}\cdot\text{cm}^{-1}$ at 762 K, which is more than twice higher than that of pure Bi₂S₃ ($12.9 \text{ S}\cdot\text{cm}^{-1}$), and Bi₂S₃ doped with 0.25mol% BiCl₃ achieves the minimum thermal conductivity of $0.31 \text{ W}\cdot\text{m}^{-1}\cdot\text{K}^{-1}$ at 762 K, more than 30% decrease as compared with pure Bi₂S₃. Due to the higher electrical conductivity and lower thermal conductivity, a maximum ZT value of 0.63 is achieved at 762 K for Bi₂S₃ doped with 0.25mol% BiCl₃, a significant enhancement compared to that of pure Bi₂S₃ (0.22).

References:

- [1] PEI Y, SHI X, LALONDE A, *et al.* Convergence of electronic bands for high performance bulk thermoelectrics. *Nature*, 2011, **473**(7345): 66–69.
- [2] BELL L E. Cooling, heating, generating power, and recovering waste heat with thermoelectric systems. *Science*, 2008, **321**(5895): 1457–1461.
- [3] DISALVO F J. Thermoelectric cooling and power generation. *Science*, 1999, **285**(5428): 703–706.
- [4] LI J F, LIU W S, ZHAO L D, *et al.* High-performance nanostructured thermoelectric materials. *NPG Asia Materials*, 2010, **2**(4): 152–158.
- [5] SNYDER G J, TOBERER E S. Complex thermoelectric materials. *Nature Materials*, 2008, **7**(2): 105–114.
- [6] YANG Y, MA F Y, LEI C H, *et al.* Is thermoelectric conversion efficiency of a composite bounded by its constituents? *Applied Physics Letters*, 2013, **102**(5): 053905–1–4.
- [7] YANG Y, XIE S H, MA F Y, *et al.* On the effective thermoelectric properties of layered heterogeneous medium. *Journal of Applied Physics*, 2012, **111**(1): 013510–1–7.
- [8] KIM W, ZIDE J, GOSSARD A, *et al.* Thermal conductivity reduction and thermoelectric figure of merit increase by embedding nanoparticles in crystalline semiconductors. *Physical Review Letters*, 2006, **96**(4): 045901–1–4.
- [9] MUTA H, IEDA A, KUROSAKI K, *et al.* Substitution effect on the thermoelectric properties of alkaline earth titanate. *Materials Letters*, 2004, **58**(30): 3868–3871.

- [10] NASR ESFAHANI E, MA F, WANG S, *et al*. Quantitative nanoscale mapping of three-phase thermal conductivities in filled skutterudites via scanning thermal microscopy. *National Science Review*, 2017, **5**(1): 59–69.
- [11] LIU Y, CHEN L, LI J. Precipitate morphologies of pseudobinary Sb₂Te₃–PbTe thermoelectric compounds. *Acta Materialia*, 2014, **65**: 308–315.
- [12] YANG Y, MA F Y, LEI C H, *et al*. Nonlinear asymptotic homogenization and the effective behavior of layered thermoelectric composites. *Journal of the Mechanics and Physics of Solids*, 2013, **61**(8): 1768–1783.
- [13] WANG C, NIU Y, JIANG J, *et al*. Hybrid thermoelectric battery electrode FeS₂ study. *Nano Energy*, 2018, **45**: 432–438.
- [14] DUGHAI SH Z H. Lead telluride as a thermoelectric material for thermoelectric power generation. *Physica B: Condensed Matter*, 2002, **322**(1/2): 205–223.
- [15] HEREMANS J P, JOVOVIC V, TOBERER E S, *et al*. Enhancement of thermoelectric efficiency in PbTe by distortion of the electronic density of states. *Science*, 2008, **321**(5888): 554–557.
- [16] POUDEL B, HAO Q, MA Y, *et al*. High-thermoelectric performance of nanostructured bismuth antimony telluride bulk alloys. *Science*, 2008, **320**(5876): 634–638.
- [17] CAO Y Q, ZHAO X B, ZHU T J, *et al*. Syntheses and thermoelectric properties of Bi₂Te₃/Sb₂Te₃ bulk nanocomposites with laminated nanostructure. *Applied Physics Letters*, 2008, **92**(14): 143106–1–3.
- [18] CANTARERO A, MARTINEZ-PASTOR J, SEGURA A, *et al*. Transport properties of bismuth sulfide single crystals. *Physical Review B*, 1987, **35**(18): 9586–9590.
- [19] BISWAS K, ZHAO L D, KANATZIDIS M G. Tellurium-free thermoelectric: the anisotropic n-type semiconductor Bi₂S₃. *Advanced Energy Materials*, 2012, **2**(6): 634–638.
- [20] LIU W, GUO C F, YAO M, *et al*. Bi₂S₃ nanonetwork as precursor for improved thermoelectric performance. *Nano Energy*, 2014, **4**: 113–122.
- [21] CHEN B, UHER C, IORDANIDIS L, *et al*. Transport properties of Bi₂S₃ and the ternary bismuth sulfides KBi_{6.33}S₁₀ and K₂Bi₈S₁₃. *Chemistry of Materials*, 1997, **9**(7): 1655–1658.
- [22] LIUFU S C, CHEN L D, YAO Q, *et al*. Assembly of one-dimensional nanorods into Bi₂S₃ films with enhanced thermoelectric transport properties. *Applied Physics Letters*, 2007, **90**(11): 112106–1–3.
- [23] GE Z H, ZHANG B P, LIU Y, *et al*. Nanostructured Bi_{2–x}Cu_xS₃ bulk materials with enhanced thermoelectric performance. *Physical Chemistry Chemical Physics*, 2012, **14**(13): 4475–4481.
- [24] YU Y Q, ZHANG B P, GE Z H, *et al*. Thermoelectric properties of Ag-doped bismuth sulfide polycrystals prepared by mechanical alloying and spark plasma sintering. *Materials Chemistry and Physics*, 2011, **131**(1/2): 216–222.
- [25] DU X, CAI F, WANG X. Enhanced thermoelectric performance of chloride doped bismuth sulfide prepared by mechanical alloying and spark plasma sintering. *Journal of Alloys and Compounds*, 2014, **587**: 6–9.
- [26] YANG X X, ZHOU Z F, WANG Y, *et al*. Raman spectroscopy determination of the Debye temperature and atomic cohesive energy of CdS, CdSe, Bi₂Se₃, and Sb₂Te₃ nanostructures. *Journal of Applied Physics*, 2012, **112**(8): 083508–1–6.
- [27] PHURUANGRAT A, THONGTEM T, THONGTEM S. Characterization of Bi₂S₃ nanorods and nano-structured flowers prepared by a hydrothermal method. *Materials Letters*, 2009, **63**(17): 1496–1498.
- [28] ZHAO L D, ZHANG B P, LIU W S, *et al*. Enhanced thermoelectric properties of bismuth sulfide polycrystals prepared by mechanical alloying and spark plasma sintering. *Journal of Solid State Chemistry*, 2008, **181**(12): 3278–3282.
- [29] ZHAO L D, LO S H, ZHANG Y, *et al*. Ultralow thermal conductivity and high thermoelectric figure of merit in SnSe crystals. *Nature*, 2014, **508**(7496): 373–377.
- [30] HAN Y M, ZHAO J, ZHOU M, *et al*. Thermoelectric performance of SnS and SnS–SnSe solid solution. *Journal of Materials Chemistry A*, 2015, **3**(8): 4555–4559.
- [31] TAN G, ZHAO L D, KANATZIDIS M G. Rationally designing high-performance bulk thermoelectric materials. *Chemical Reviews*, 2016, **116**(19): 12123–12149.
- [32] GE Z H, QIN P, HE D S, *et al*. Highly enhanced thermoelectric properties of Bi/Bi₂S₃ nanocomposites. *ACS Applied Materials & Interfaces*, 2017, **9**(5): 4828–4834.
- [33] YANG J, LIU G, YAN J, *et al*. Enhanced the thermoelectric properties of n-type Bi₂S₃ polycrystalline by iodine doping. *Journal of Alloys and Compounds*, 2017, **728**: 351–356.
- [34] ZHANG L J, ZHANG B P, GE Z H, *et al*. Fabrication and properties of Bi₂S_{3–x}Se_x thermoelectric polycrystals. *Solid State Communications*, 2013, **162**: 48–52.

水热合成 $\text{BiCl}_3/\text{Bi}_2\text{S}_3$ 复合材料的热电性能

王伟¹, 罗世阶¹, 鲜聪¹, 肖群¹, 杨洋², 欧云³, 刘运牙¹, 谢淑红⁴

(1. 湘潭大学 材料科学与工程学院 湖南省薄膜材料与器件重点实验室, 湘潭 411105; 2. 华盛顿大学 机械工程系, 西雅图 WA98195-2600, 美国; 3. 湖南科技大学 机械设备健康维护湖南省重点实验室, 湘潭 411201; 4. 湘潭大学 低维材料与应用技术教育部重点实验室, 湘潭 411105)

摘要: 采用水热合成法制备了由纳米棒组成的微米级球形 Bi_2S_3 颗粒, 然后通过放电等离子烧结技术(SPS)将不同摩尔比例的 $\text{BiCl}_3/\text{Bi}_2\text{S}_3$ 复合粉末制备成块体。加入适量的 BiCl_3 不仅提高了 Bi_2S_3 样品的导电率, 而且降低了其热导率。 Bi_2S_3 复合 0.5mol% BiCl_3 的样品在 762 K 电导率最大, 达到 $45.1 \text{ S}\cdot\text{cm}^{-1}$, 远高于此温度下纯 Bi_2S_3 样品的电导率($12.9 \text{ S}\cdot\text{cm}^{-1}$)。 Bi_2S_3 复合 0.25mol% BiCl_3 的样品在 762 K 时热导率最低, 为 $0.31 \text{ W}\cdot\text{m}^{-1}\cdot\text{K}^{-1}$, 低于同一温度下纯 Bi_2S_3 的 $0.47 \text{ W}\cdot\text{m}^{-1}\cdot\text{K}^{-1}$ 。在 762 K 下, Bi_2S_3 复合 0.25mol% BiCl_3 的样品获得最大 ZT 值(0.63), 比纯 Bi_2S_3 样品(0.22)提高了大约 2 倍。

关键词: Bi_2S_3 ; 水热法; 球形颗粒; 放电等离子烧结; 热电

中图分类号: TB34 文献标识码: A